In vivo high-resolution magic angle spinning magnetic and electron paramagnetic resonance spectroscopic analysis of mitochondria-targeted peptide in *Drosophila melanogaster* with trauma-induced thoracic injury

CATERINA CONSTANTINOU[1,2,8], YIORGOS APIDIANAKIS[2], NIKOLAOS PSYCHOGIOS[1,3], VALERIA RIGHI[1,3], MICHAEL N. MINDRINOS[4], NADEEM KHAN[5], HAROLD M. SWARTZ[5], HAZEL H. SZETO[6], RONALD G. TOMPKINS[7], LAURENCE G. RAHME[2] and A. ARIA TZIKA[1,3]

[1]NMR Surgical Laboratory and [2]Molecular Surgery Laboratory, Center for Surgery, Innovation and Bioengineering, Department of Surgery, Massachusetts General Hospital and Shriners Burns Institute, Harvard Medical School; [3]Department of Radiology, Massachusetts General Hospital, Harvard Medical School, Athinoula A. Martinos Center for Biomedical Imaging, Boston, MA; [4]Department of Biochemistry, Stanford University School of Medicine, Stanford, CA; [5]EPR Center for Viable Systems, Department of Diagnostic Radiology, The Geisel School of Medicine, Lebanon, NH; [6]Department of Pharmacology, Joan and Sanford I. Weill Medical College of Cornell University, New York, NY; [7]Center for Surgery, Innovation and Bioengineering, Department of Surgery, Massachusetts General Hospital, Harvard Medical School, Boston, MA, USA

Received July 9, 2015; Accepted October 29, 2015

DOI: 10.3892/ijmm.2015.2426

Abstract. Trauma is the most common cause of mortality among individuals aged between 1 and 44 years and the third leading cause of mortality overall in the US. In this study, we examined the effects of trauma on the expression of genes in *Drosophila melanogaster*, a useful model for investigating genetics and physiology. After trauma was induced by a non-lethal needle puncture of the thorax, we observed the differential expression of genes encoding for mitochondrial uncoupling proteins, as well as those encoding for apoptosis-related and insulin signaling-related proteins, thus indicating muscle functional dysregulation. These results prompted us to examine the link between insulin signaling and mitochondrial dysfunction using *in vivo* nuclear magnetic resonance (NMR) with complementary electron paramagnetic resonance (EPR) spectroscopy. Trauma significantly increased insulin resistance biomarkers, and the NMR spectral profile of the aged flies with trauma-induced thoracic injury resembled that of insulin-resistant *chico* mutant flies. In addition, the mitochondrial redox status, as measured by EPR, was significantly altered following trauma, indicating mitochondrial uncoupling. A mitochondria-targeted compound, Szeto-Schiller (SS)-31 that promotes adenosine triphosphate (ATP) synthesis normalized the NMR spectral profile, as well as the mitochondrial redox status of the flies with trauma-induced thoracic injury, as assessed by EPR. Based on these findings, we propose a molecular mechanism responsible for trauma-related mortality and also propose that trauma sequelae in aging are linked to insulin signaling and mitochondrial dysfunction. Our findings further suggest that SS-31 attenuates trauma-associated pathological changes.

Correspondence to: Dr A. Aria Tzika, NMR Surgical Laboratory, Department of Surgery, Massachusetts General and Shriners Burns Institute, Harvard Medical School, 51 Blossom Street, Room 261, Boston, MA 02114, USA
E-mail: atzika@hms.harvard.edu

Present address: [8]Pharmacology Unit, Department of Medicine, University of Patras, Rio Achaias 26500, Greece

Abbreviations: Ac, acetate; Ala, alanine; β-Ala, β-alanine; Arg, arginine; CPMG, Carr-Purcell-Meiboom-Gill; EMCLs, extramyocellular lipids; FID, free induction decay; ^{1}H-NMR, proton nuclear magnetic resonance; HRMAS, high-resolution magic angle spinning; EPR, electron paramagnetic resonance; IMCLs, intramyocellular lipids; NMR, nuclear magnetic resonance; PE, phosphoethanolamine; PC, phosphocholine; PUFA, polyunsaturated fatty acid; ROS, reactive oxygen species; SS-31, Szeto-Schiller-31; Tau, taurine; TG, triglycerides; wt, wild-type

Key words: nuclear magnetic resonance, electron paramagnetic resonance, high-resolution magic angle spinning, mitochondria, *Drosophila melanogaster*, biomarkers, insulin signaling, aging

Introduction

The annual mortality rate due to traumatic injury in the US is approximately 192,000 individuals annually, while unintentional injuries are ranked among the top 10 causes of mortality in adults 65 years of age and older, of both genders (http://www.

nationaltraumainstitute.org/home/trauma_statistics.html). The leading complication associated with trauma is the onset of several pathological pathways which leads to multiple-organ failure several days post-injury (1).

Since aging is characterized by increased oxidative stress, a heightened inflammatory response, accelerated cellular senescence and progressive organ dysfunction, it has been proposed that the homeostatic imbalance with aging significantly alters cellular responses to injury (2). In particular, previous research on aging has shown alterations in the levels or activity of factors involved in key regulatory processes in the maintenance of mitochondrial structural integrity, biogenesis and function, thus leading to the hypothesis that the cellular energetic imbalance may be important for the restoration of organ function following severe injury in aged individuals (3). That is, with severe insults, the mitochondrion, which plays a pivotal role in healthy aging (2) and, consequently, in the physiological response to trauma and shock (4), becomes stressed and eventually, dysfunctional. The most serious consequences of mitochondrial dysfunction are realized when ATP production falters. The inhibition of mitochondrial respiration leads to compromised ATP production and increased levels of reactive oxygen species (ROS) due to electron leakage. Mitochondrial oxidative stress damages cellular and mitochondrial protein machinery and genomic DNA, thereby compromising the repair and recovery capacities of the body. Furthermore, Jacob *et al*, using proton nuclear magnetic resonance (^{1}H-NMR) spectroscopy, demonstrated that a high intramyocellular lipid (IMCL) content is exhibited early in the pathogenesis of insulin resistance, highlighting the importance of the IMCL content as a biomarker of insulin resistance in patients with type 2 diabetes and their offspring (5). Indeed, the IMCL content in the soleus muscle has been found to be increased in insulin-resistant elderly patients, thus providing support for the hypothesis that an age-associated decline in mitochondrial function contributes to insulin resistance (6).

High-resolution magic angle spinning (HRMAS) ^{1}H-NMR spectroscopy is a novel non-invasive technique that yields substantially improved spectral line-widths compared to conventional NMR, and therefore facilitates the acquisition of high-resolution spectra from intact cells (7,8) and unprocessed tissue (9-12). Although HRMAS ^{1}H-NMR allows the associations between metabolites, such as IMCLs, and cellular processes to be investigated more closely than previously possible, it is generally performed *ex vivo* (13). Szczepaniak *et al* recently demonstrated that the IMCL content can be quantified accurately in a clinical setting with *in vivo* ^{1}H-NMR spectroscopy (14). In the present study, for the first time and to the best of our knowledge, we applied the emergent *in vivo* HRMAS proton magnetic resonance spectroscopy (^{1}H-MRS) methodology to *Drosophila* in order to examine the effects of trauma-induced injury. We anticipated that *in vivo* HRMAS ^{1}H-NMR would be a useful tool in *Drosophila* since *in vitro* NMR can be used to demonstrate the metabolic effects of hypoxia (15) and temperature stress (16) in flies. *Drosophila melanogaster* (*D. melanogaster*), a small, short-lived and genetically amenable model organism with mutants for several genes of interest, already available, provides a useful model tool for assessing the biomarkers of trauma pathophysiology and for providing critical information on the development of novel therapies for trauma in a systemic and systematic manner. In addition, a range of antioxidant defenses has evolved in *Drosophila*, protecting the flies against impending oxidative damage, including antioxidant enzymes (e.g., superoxide dismutase, catalase and glutathione reductase) that suppress ROS activity before ROS can damage the vital cellular components (16,17). Although there is a lack of strong links between antioxidant enzymes and normal aging, antioxidant enzymes play an important role in extending the longevity of *Drosophila* under stressful conditions (17). Therefore, assessing the redox status of the mitochondria in injured flies is a rational means of evaluating the antioxidant defense capabilities of the flies.

The present study was designed to examine the hypothesis that trauma leads to reduced insulin signaling, a phylogenetically conserved pathway for the regulation of glucose and lipid metabolism (18,19), and mitochondrial dysfunction. Insulin signaling was assessed by cDNA microarrays, insulin resistance was evaluated by the *in vivo* assessment of the IMCL content, and mitochondrial dysfunction was evaluated by estimating *in vivo* ROS production. Finally, we examined whether the Szeto-Schiller (SS)-31 peptide, which is known to interact specifically with cardiolipin, and prevents the conversion of cytochrome *c* into a peroxidase while promoting oxidative phosphorylation (20), can reverse these effects. This hypothesis was examined in aged flies with trauma-induced injury which were injected with saline or SS-31. *In vivo* HRMAS ^{1}H-NMR and electron paramagnetic resonance (EPR) spectroscopy were applied to eliminate the *in vitro* artifacts.

Materials and methods

Flies. Aged male *D. melanogaster* flies (age range, 30-33 days) weighing 0.7-1.0 mg were used in all the experiments. Oregon-R flies (wild type) were obtained from the Bloomington Drosophila Stock Center, Department of Biology, Indiana University, IN, USA. For the microarray genome analysis, wild-type (wt) flies were used, and the gene expression in flies injured with a thoracic non-lethal, needle puncture, as previously described (21,22), was compared to that in uninjured control flies. *In vivo* HRMAS ^{1}H-NMR spectroscopy was conducted on 3 groups of flies (n=6 per group). The 3 groups of flies were as follows: a) uninjured wt flies; b) wt flies injured 24 h prior to examination; and c) injured wt flies injected with SS-31 12 h post-injury. SS-31 (3 mg/kg) was injected into the thorax, using a Nanojet II injector (Drummond Scientific, Broomall, PA, USA) at 0, 3, 6, 24 and 48 h after needle puncture injury, as described in the study by Apidianakis and Rahme (22). The flies in groups 'a' and 'b' received injections of saline only following the same schedule, and a group of uninjured control flies was injected with SS-31 in order to determine the effects of the agent alone in the absence of trauma. To demonstrate that the HRMAS ^{1}H-NMR spectra obtained from whole flies are similar to those of muscle-enriched fly thoraces, we also analyzed dissected thoraces from 6 flies. Fly heads, abdomens and legs were removed from the flies and the thoraces were preserved on ice for 2-6 h prior to their analysis. In our other experiments, only whole flies were used.

EPR spectroscopy to investigate the redox status was also conducted on the same groups of flies as used in the

HRMAS ^{1}H-NMR spectroscopy experiments. For the *in vivo* HRMAS ^{1}H-NMR and EPR spectroscopy experiments, we also assessed *chico*$^{1/2}$ flies (kindly donated by Dr Robert Perrimon, Department of Genetics, Harvard Medical School, Boston, MA, USA), bearing 2 mutated alleles of the *chico* gene, a *Drosophila* homolog of vertebrate insulin receptor substrate 1-4 (IRS1-4), and their genetic control, *chico*$^{1/+}$ flies, were also used, as previously described (23). Naïve *chico*$^{1/2}$ mutant flies were used as the controls for the injured flies.

Microarray hybridization and genomic data analysis. Biotinylated cRNA was generated with 10 μg of total cellular RNA from the wt flies according to the protocol outlined by Affymetrix, Inc. (Santa Clara, CA, USA). cRNA was hybridized onto an Affymetrix GeneChip® *Drosophila* Genome oligonucleotide array (Affymetrix, Inc.), labeled with streptavidin-phycoerythrin, washed and scanned according to the manufacturer's instructions.

Data files of the scanned images of the arrays hybridized with probes from the RNA extracted from *Drosophila* muscle isolated at the specified time points from the flies with trauma-induced thoracic injury and the control flies (n=3/group per time point) were converted to cell intensity files (.CEL files) in the Microarray Suite 5.0 program (MAS; Affymetrix). The data were scaled to a target intensity of 500, and all possible pairwise array comparisons of the replicates (injured vs. uninjured control flies) were performed for each time point using a MAS 5.0 change call algorithm. Probe sets that had a signal value difference >100, and for which one of the two samples being compared was not assessed as 'absent', were scored as differentially modulated when the following two conditions were met: i) the number of changes registered in the same direction were at least 3, 4 and 6, when the number of comparisons were 4, 6 and 9, respectively; and ii) the other comparisons were unaltered. This scoring method compensates partially for biological stochasticity and technical variation. Based on the ratios of 100 genes determined to be invariant in the majority of conditions tested (Affymetrix), an additional constraint of a minimum ratio of 1.65 was applied in order to control for known false-positives at a level of 5%.

To identify functionally related sets of genes and processes significantly associated with trauma (at $p \leq 0.05$), we used the GeneSpring tool to characterize the genes found to be differentially expressed in the flies with trauma-induced thoracic injury compared to the control flies and compared to the Gene Ontology Consortium database. The microarray data are available online at MIAMExpress (accession no. E-MEXP-1287). The expression levels of all presented genes were verified by reverse transcription-quantitative polymerase chain reaction experiments (data not shown).

In vivo HRMAS ^{1}H-NMR spectroscopy. All HRMAS ^{1}H-NMR spectroscopy experiments were performed on a wide-bore Bruker Bio-Spin Avance NMR spectrometer (600.13 MHz) using a 4-mm triple resonance (^{1}H, ^{13}C and ^{2}H) HRMAS probe (both from Bruker Corp., Billerica, MA, USA). Prior to being placed in the spectrometer, each fly was anesthetized by being set on ice for <1 min. The flies were kept at 4˚C while in the spectrometer. Special care was taken to avoid inflicting further injury on the already injured flies as they were moved in and out of the rotor. All flies survived the HRMAS ^{1}H-NMR spectroscopy experiment, which lasted ~45 min for each fly.

The flies were placed individually into a zirconium oxide (ZrO_2) rotor tube (Bruker BioSpin Corp., Bruker BioSpin AG, Billerica, MA, USA; 4 mm in diameter, 50 μl), and 8 μl of external standard 3-(trimethylsilyl) propionic-2,2,3,3-d4 acid (TSP), (molecular weight, 172, δ=0.00 ppm, 50 mM in D_2O) that functioned as a reference for both resonance chemical shift and quantification, was then pipetted into each tube. Each fly was placed in the rotor using the insert, and the insert was then closed with a screw and covered with parafilm to prevent contact between the fly and the TSP/D_2O. The samples were secured and tightened in the rotors with a top cap (Bruker Corp.). HRMAS ^{1}H-NMR spectroscopy was performed at 4˚C with a spinning frequency of 2 kHz.

One dimensional (1D) water-suppressed spin-echo Carr-Purcell-Meiboom-Gill (CPMG) pulse sequence [90˚-(τ-180˚-τ)$_n$-acquisition] (24) was performed on single flies. CPMG is a methodological improvement which is of particular relevance when developing HRMAS for intact tissue samples *ex vivo* in 1D acquisition, since it suppresses broad signals that destroy the linear baseline in typical free induction decay (FID) spectra. As a result, CPMG proton NMR spectra are free from the broad 'rolling' component that contributes to the baseline of simple FID spectra. The CPMG sequence has also been applied to 2 dimensional (2D) sequences for the same reason. Additional parameters for the CPMG sequence included an inter-pulse delay of $\tau = 2\pi/\omega_r = 250$ μsec, two 180˚ cycles in total, 256 transients, a spectral width of 7.2 kHz, 32,768 (32 k) data points, and a 3-sec repetition time. We selected a spin-echo delay of 30 msec as we observed that it enabled us to avoid line broadening without the loss of signals from triglycerides (TG). A longer spin-echo delay improved all lipid signals, but was not favorable to other metabolite signals.

^{1}H HRMAS NMR spectroscopy data processing. NMR spectra were analyzed with MestReC software (Mestrelab Research, www.mestrec.com). A 0.5-Hz line-broadening apodization function was applied to CPMG HRMAS ^{1}H FIDs prior to Fourier transformation. The spectra were referenced relative to TSP at δ=0.0 ppm (external standard), manually phased, and a Whittaker baseline estimator was applied to subtract the broad components of the baseline.

Quantification of metabolites from 1D CPMG spectra. For metabolite quantification, we used the highly accurate 'external standard' technique. Metabolite concentrations were calculated using MestReC software. An automated fitting routine based on the Levenberg-Marquardt algorithm (25,26) was applied following manual peak selection; peak positions, intensities, line widths and Lorentzian/Gaussian ratios were adjusted until the residual spectrum was minimized. The metabolite concentration (mol/kg) was calculated using the following equation, as previously described (27): $mass_{TSP}/PM_{TSP} * Met_{(area)}/TSP_{(area)} * N_{TSP}/N_{Met} * 1/wt$ (sample), where $mass_{TSP}$ was constant (0.069 mg), PM_{TSP} was the molecular weight of TSP (172.23 g/mol), Met signified metabolites, NTSP denoted the TSP proton number (9 ^{1}H), N_{Met} denoted the metabolite proton number, and wt signified the sample weight in mg (27).

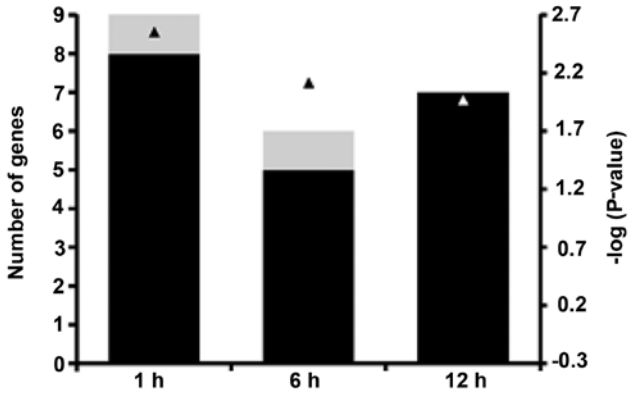

Figure 1. Differentially expressed genes with electron transport-related functionality in injured flies, as identified using Gene Ontology at p≤0.05. At each time point, the gray and black bars indicate the numbers of upregulated and downregulated genes, respectively. The negative $\log_{10}$-transformed p-values (right y-axis) are represented by triangles.

EPR spectroscopy for post-trauma redox assessment. X-band EPR with nitroxide was implemented as a complementary approach to NMR since NMR cannot measure the redox status (28,29). For redox assessment, each fly was anesthetized by cooling on ice (4˚C) for 1 min and 9.2 nl of 15 mg/kg 2,2,6,6-tetramethylpiperidine 1-oxyl (TEMPO; Sigma-Aldrich, St. Louis, MO, USA) was then injected into the abdomen via an automated microsyringe, as previously described (22). Due to the very small size of *Drosophila* and in order to minimize repetitive injury, TEMPO was injected into each fly only once. Therefore, we used different flies for redox measurements at each time point. The anesthetized flies were quickly transferred to the EPR sample tube (1/tube) and restrained gently between cotton plugs to minimize any motion during the measurements. The EPR sample tube was then placed in the cavity of the Bruker X-band 9.2-GHz EPR spectrometer to follow the decay of the nitroxide (TEMPO) for 10-15 min. This method allowed us to assess the redox status of the flies directly, using an X-band EPR spectrometer as previously described (28-30).

Typical spectrometer parameters were as follows: incident microwave power, 0.5 mW; magnetic field center, 348.7 mT; modulation frequency, 100 kHz; modulation amplitude, 40 μT; scan width, 1.5 mT and a scan time of 10 sec/scan. The low-field component of the EPR spectra (i.e., the first EPR line) was averaged over 1 min, and changes in signal intensity were followed over time. The rate at which the nitroxide was reduced over time was taken as an index of the redox status of the flies. In a previous study, we used a similar procedure to examine the redox status of muscle in mice following burn injury (30). After the redox measurement, the flies were gently removed from the tubes and transferred to Eppendorf tubes to follow their survival.

Statistical analysis. Statistical comparisons were carried out using analyses of variance (ANOVA) with the Bonferroni correction to account for multiple of comparisons. A p-value <0.05 (corrected) was considered to indicate a statistically significant difference; p-values are reported to two significant digits. Calculations were performed using SPSS version 12 software (SPSS Inc., Chicago, IL, USA).

Results

Gene expression. The analysis of Affymetrix microarrays identified 245, 187 and 191 genes as differentially expressed in whole flies at 1, 6 and 12 h post-trauma. Our comparison of these sets of differentially expressed genes to the Gene Ontology Consortium database pointed to electron transport being the predominant function affected by trauma; the number of electron transport-related genes whose expression was abnormal at each time point is shown in Fig. 1.

As shown in Fig. 2, trauma affected the expression of several genes related to mitochondrial function across multiple time points. As expected, the expression of genes encoding

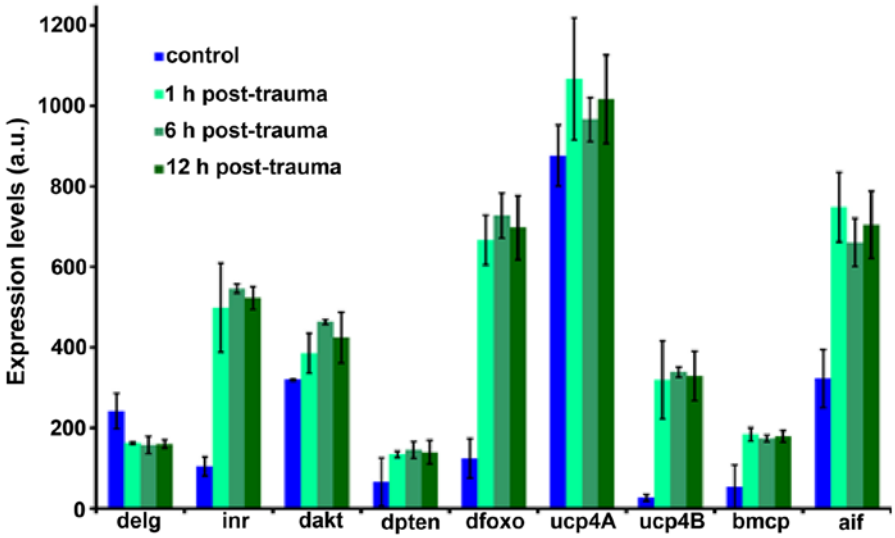

Figure 2. Changes in mitochondrial function-related gene mRNA expression in flies at 1, 6 and 12 h post-trauma. Expression levels are reported in arbitrary units (a.u.). delg, *Drosophila* NRF-2; inr, *Drosophila* insulin receptor; dakt, *Drosophila* AKT; dpten, *Drosophila* phosphatase and tensin homolog; dfoxo, *Drosophila* Forkhead box O; ucp4A, uncoupling protein4A; ucp4b, uncoupling protein4b; bmcp, drosophila ucp5; aif, apoptosis-inducing factor.

for mitochondrial uncoupling protein UCP4 (*ucp*) was highly upregulated. Additionally, we observed an upregulation in the expression of genes encoding for apoptosis-inducing factor (*aif*) and *Drosophila* Forkhead box O (*dfoxo*). We also observed the altered expression of genes encoding for *Drosophila* insulin receptor (*inr*), *Drosophila* AKT (*dakt*), and *Drosophila* phosphatase and tensin homolog (*dpten*), which indicates trauma-induced insulin signaling dysregulation; this insulin signaling dysregulation may be linked to the downregulation of *Drosophila* Ets-like gene (*delg*) that was also observed. These findings prompted us to examine the link between mitochondrial dysfunction and insulin signaling in an *in vivo* model using *in vivo* NMR and EPR.

In vivo 1D ^{1}H HRMAS. Representative *in vivo* 1D ^{1}H HRMAS CPMG spectra from uninjured aged wt flies, injured aged wt flies and *chico*$^{1/2}$ mutants are illustrated in Fig. 3 together with a 1D ^{1}H HRMAS CPMG summed spectrum from the thorax of dissected wt flies (inset), which represents primarily skeletal muscle, as the fly thorax is highly enriched in skeletal muscle, demonstrating that the spectra from whole flies are similar to those from the muscle-enriched thorax. Principal lipid components [CH_3 (0.89 ppm), (CH_2)n (1.33 ppm), CH_2C-CO (1.58 ppm), CH_2C=C (2.02 ppm), CH_2C=O (2.24 ppm), CH=CH (5.33 ppm)], glycerol (4.10, 4.30 and 5.24 ppm), acetate (Ac, 1.92 ppm), β-alanine (β-Ala, 2.55 ppm), phosphocholine (PC, 3.22 ppm) and phosphoethanolamine (PE, 3.22 ppm)] were detected. Signals at 2.02 ppm were assigned to methylene protons of the CH_2-CH=CH moiety of monounsaturated fatty acids (i.e., palmitoleic acid). Of note, we detected increased levels of polyunsaturated fatty acids (PUFAs, CH_2C=O at 2.24 ppm). The unsaturated acids were identified by a signal at 5.33 ppm produced by protons of the -CH=CH- moiety.

The metabolic HRMAS NMR profiles of the injured aged wt flies were similar to those of the *chico*$^{1/2}$ mutants (Fig. 3). The SS-31 injection normalized the NMR profiles of the injured aged wt flies (Fig. 4**).** Quantitative analysis revealed significant increases in (CH_2)n lipids at 1.33 ppm (an insulin resistance biomarker) and CH=CH lipids at 5.33 ppm (an apoptosis biomarker) in the injured aged wt flies compared to the uninjured aged wt flies (Table I). The majority of the other lipid resonances were significantly elevated in the injured flies compared to the uninjured flies. The levels of the (CH_2)n and CH=CH lipids were normalized in the injured flies injected with SS-31 (Table I).

Analysis of the transverse relaxation time, T_2, of the metabolites and the TSP standard in the 1D ^{1}H CPMG spectra across echo times (TE at 30, 60, 100, 300, 450 and 600 msec) revealed that the T_2 decay rate for the -CH_3 groups at 0.89 ppm (1,156±72 msec) was very close to that of TSP (1,125±103 msec). The T_2 values for (CH_2)n at 1.33 ppm (516±14 msec), CH_2C=C at 2.02 ppm (537±35 msec) and CH=CH at 5.33 ppm (469±27 msec) were almost identical to each other, equating to approximately half the T_2 values for CH_2CCO at 1.58 ppm (292±5.0 msec) and CH_2CO at 2.24 ppm (265±16 msec). Even at TE=600 ms, these peaks were not completely decayed, indicating that the lipid relaxation kinetics resembled those of TSP.

EPR spectroscopy. The typical *in vivo* X-band EPR spectra acquired from the flies is illustrated in Fig. 5A. Our

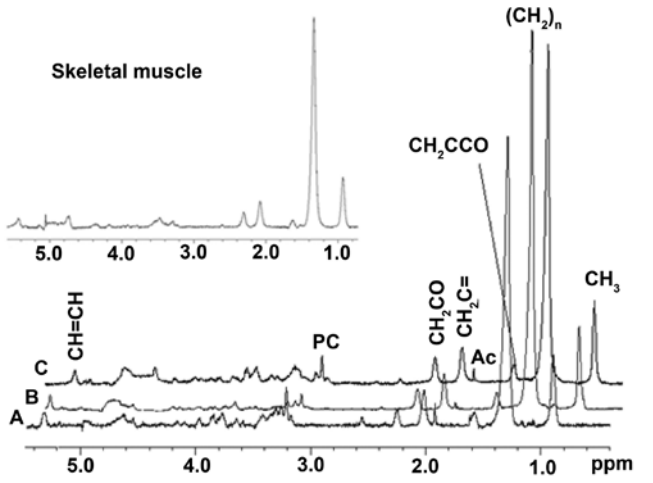

Figure 3. Representative *in vivo* 1D HRMAS ^{1}H CPMG spectra of (A) uninjured aged wild-type (wt) flies, (B) injured old wt flies and (C) chico$^{1/2}$ mutants. Lipid components: CH_3 (0.89 ppm), (CH_2)n (1.33 ppm), CH_2C-CO (1.58 ppm), acetate (Ac, 1.92 ppm), CH_2C=C (2.02 ppm), CH_2C=O (2.24 ppm), β-alanine (β-Ala, 2.55 ppm), phosphocholine (PC, 3.22 ppm), and phosphoethanolamine (PE, 3.22 ppm), glycerol (4.10, 4.30 ppm 1,3-CH; 5.22 ppm 2-CH_2), CH=CH (5.33 ppm). Note that spectra from *chico*$^{1/2}$ mutants with insulin resistance have increased insulin biomarker (CH_2)n, and that the spectra from injured wt flies have a similar profile. The spectra in the insert are from the thorax of dissected flies and thus represent primarily skeletal muscle; note their similarity to spectra for whole flies.

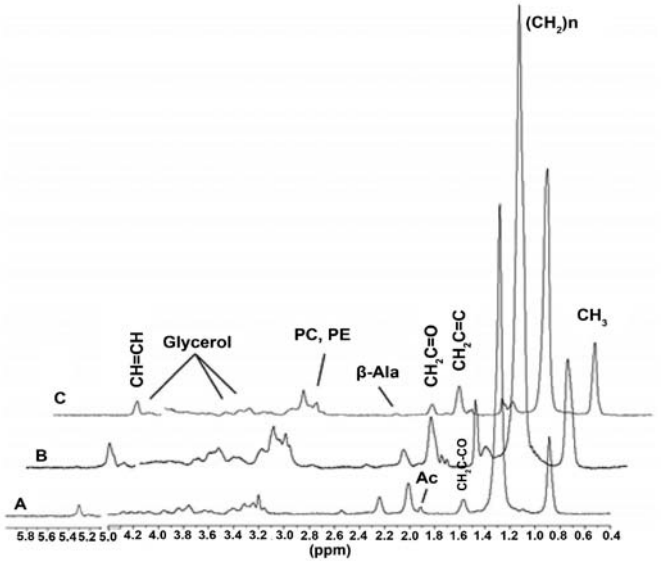

Figure 4. Representative summed *in vivo* 1D HRMAS ^{1}H CPMG spectra of (A) uninjured aged wild-type (wt) flies and (B) injured aged wt flies, (C) injured aged wt flies treated with Szeto-Schiller (SS)-31. Lipid components: CH_3 (0.89 ppm), (CH_2)n (1.33 ppm), CH_2C-CO (1.58 ppm), acetate (Ac, 1.92 ppm), CH_2C=C (2.02 ppm), CH_2C=O (2.24 ppm), β-alanine (β-Ala, 2.55 ppm), phosphocholine (PC, 3.22 ppm), phosphoethanolamine (PE, 3.22 ppm), glycerol (4.10, 4.30 ppm 1,3-CH; 5.22 ppm 2-CH_2), and CH=CH (5.33 ppm). Note that injured flies injected with SS-31 (C) have a profile that is similar to that of the uninjured old wt flies (A).

minute-by-minute analysis of the changes in the low field component of the TEMPO nitroxide (Fig. 5B) indicated that the redox status was compromised in the flies at 1 and 6 h post-injury. The redox status (Kr) in the injured flies at 1 and 6 h post-injury was 0.0187±0.0040/sec and 0.0187±0.0043/sec, respectively, and did not differ significantly between these two

Table I. Mean quantity (in μmol/g ± standard errors) of selected lipid components in live wt flies determined by ^{1}H HRMAS NMR.

Time	Lipid components Chemical shift (δ, ppm)	CH_3 0.89	$(CH_2)n$ 1.33	CH_2CCO 1.58	$CH_2C=$ 2.02	CH_2CO 2.24	CH=CH 5.33
6 h	Uninjured	0.18±0.01	1.41±0.08	0.06±0.003	0.13±0.01	0.07±0.01	0.08±0.01
	Injured	0.27±0.03	2.10±0.25	0.16±0.08	0.24±0.06	0.13±0.03	0.13±0.02
	% change	50.0	48.94	166.67	84.62	85.71	62.50
	p-value	**0.022**	**0.024**	0.260	0.085	0.071	**0.015**
12 h	Injured + saline	0.26±0.003	1.94±0.05	0.13±0.01	0.22±0.004	0.10±0.01	0.13±0.004
	Injured + SS31	0.17±0.002	1.29±0.02	0.06±0.002	0.12±0.002	0.06±0.001	0.08±0.002
	% change	-33.38	-33.43	-54.95	-44.09	-45.05	-39.90
	p-value	**<0.001**	**<0.001**	**0.0013**	**< 0.001**	**< 0.001**	**< 0.001**

The p-values were calculated using ANOVA with Bonferroni correction to account for multiple comparisons. Significant p-values are shown in bold. HRMAS, high-resolution magic angle spinning; wt, wild-type; NMR, nuclear magnetic resonance.

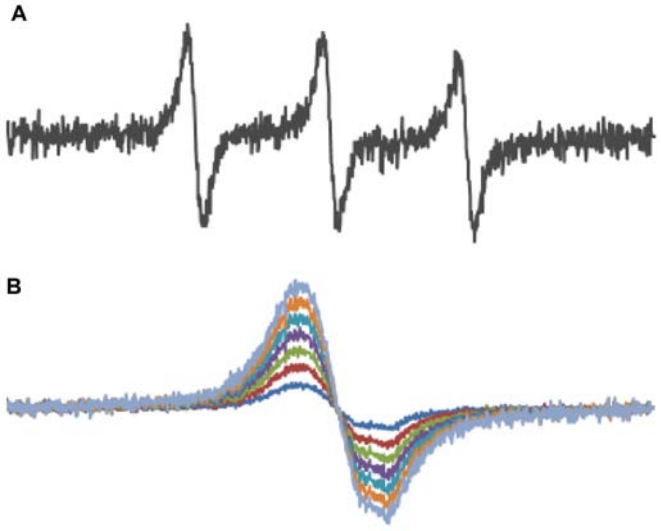

Figure 5. (A) Typical *in vivo* electron paramagnetic resonance (EPR) spectra of TEMPO-injected in the control flies. (B) The first component of the EPR spectrum was used to follow nitroxide reduction over time for evaluating redox status. Values are represented as the means ± SD; n=6/group.

time points. However, these redox measures were significantly higher than those observed in the uninjured flies in the control group (0.0131±0.0027/sec; p=0.018 vs. 1 h post-injury and p=0.024 vs. 6 h post-injury). Treatment with SS-31 significantly decreased the nitroxide decay rate at 6 h post-injury to 0.0130±0.0036/sec (p=0.040) vs. injured flies not treated with SS-31 at 6 h post-injury), a level similar to that of the uninjured control group (p=0.933).

Discussion

In the present study, we examined the link between insulin signaling and mitochondrial dysfunction following trauma by combining genomic analysis with *in vivo* 1D ^{1}H HRMAS and EPR spectroscopy in *Drosophila*. The expression of electron transport protein genes, in particular, was substantially altered in the flies with trauma-induced injury. This pattern of change is indicative of mitochondrial dysfunction following trauma and is in agreement with the findings of a previous study of ours on burn-associated trauma (31). Also consistent with our prior findings in relation to burn trauma (32), we observed the upregulation of *aif*, *dfoxo*, as well as genes related to mitochondrial uncoupling. Furthermore, we were intrigued to find the altered expression of the insulin signaling-related genes, *inr*, *dakt*, and *dpten*, which is also consistent with our murine burn trauma model (33), as well as the downregulation of *delg*, which could be a downstream effect of insulin signaling dysregulation.

The results of our subsequent *in vivo* HRMAS ^{1}H-NMR and EPR experiments support the hypothesis that trauma can reduce insulin signaling through a mechanism that involves a phylogenetically conserved pathway for the regulation of glucose and lipid metabolism (18,19), and that SS-31 can promote the recovery of mitochondrial function and alleviate this condition. Our findings broaden those of prior reports using HRMAS ^{1}H-MRS in *Drosophila* (34), and provide evidence for the hypothesis that trauma in aging is linked to dysregulated insulin signaling. This link may explain the mitochondrial dysfunction that accompanies insulin resistance in trauma and aging in mammals.

Specifically, using *in vivo* HRMAS ^{1}H-NMR (14.1 T), we detected lipids and small metabolites in live *Drosophila*. At 14.1-T, we were able to achieve a sufficiently brief acquisition time (~45 min) to attain zero mortality. In accordance with other previously published *in vivo* skeletal muscle spectra (35-37), our *in vivo* fly spectra exhibited high amounts of lipids (particularly TG), but fewer metabolites than described in certain other studies (38,39). Relative to these previous studies, we were working with a smaller sample size and using a lower spin rate, which may have affected spectral resolution. Given the low body weight of the fruit fly, NMR-visible non-lipid components are expected to contribute only a small percentage of the total signal, with a concomitantly weaker sensitivity of detection. Indeed, even spectra from the muscle-dense thorax of dissected flies were similar to the spectra from whole flies (inset of Fig. 3).

The current thinking is that, following trauma, the disruption of oxidative homeostasis, the overproduction of ROS and the opening of the mitochondrial permeability transition pore promote mitochondrial dysfunction, leading to the activation of

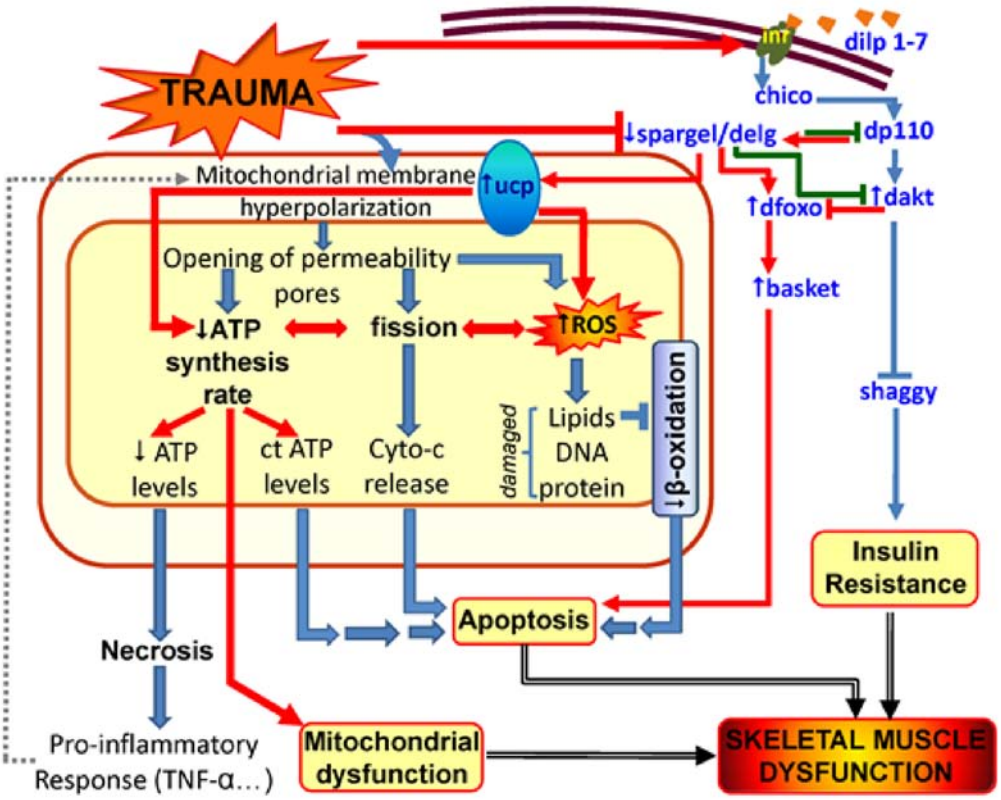

Figure 6. Proposed molecular mechanism of trauma-induced skeletal muscle dysfunction. Red lines/arrows, aspects of trauma-induced mitochondrial dysfunction suggested by our data. Green lines, proposed negative feedback mechanism of *spargel* in the insulin pathway. Blue arrows, aspects of trauma-induced mitochondrial dysfunction established previously in the literature (18-19,40-46). ct, stable; *spargel*, PGC-1 analogue in flies; delg, NRF-2 analogue in flies; ucp, uncoupling proteins; dfoxo, Forkhead box O anologue in flies; basket, JNK analogue in flies; dilp 1-7, analogues of insulin, IGF-1 and IGF-2 in flies; inr, *Drosophila* insulin receptor; chico, IRS 1-4 analogue in flies; dp110, PI3K analogue in flies; dakt, *Drosophila* AKT analogue in flies; shaggy, GSK-3 (glycogen synthase kinase-3) analogue in flies; ROS, reactive oxygen species; Cyto-*c*, cytochrome *c*; ATP, adenosine triphosphate; TNF-α, tumor necrosis factor-α.

necrotic and/or apoptotic cell death pathways (4). Based on our present findings, we propose that trauma affects mitochondrial function through the disruption of insulin signaling, which is related to the altered expression of *delg* [the *Drosophila* homologue of the α subunit of nuclear factor (erythroid-derived 2)-related factor-2 (NRF-2α)] and *spargel* (the *Drosophila* homologue of peroxisome proliferator-activated receptor-γ coactivator 1).

In light of our present findings (summarized in Fig. 6) and other evidence in the literature (40), suggesting that Spargel mediates transcription in response to insulin signaling in parallel with Dfoxo, it is important to determine whether Spargel mediates a negative feedback loop in insulin signaling that enables it to set a threshold for insulin signaling in the control of metabolism. Whilst Spargel is not necessary for the maintenance of basal mitochondrial mass under normal physiological conditions, it becomes necessary in the absence of Delg, the fly homologue of NRF-2a (40). The loss of function of both Spargel and Delg leads to a greater loss of mitochondrial mass than the loss of Delg alone (40,41), suggesting that the two factors may act in parallel. Additionally, our previously published studies (30-35,42-45), and the current findings, are consistent with the possibility that Spargel promotes mitochondrial dysfunction via uncoupling proteins; experiments testing this possibility are currently in progress.

From a biomedical perspective, a principal finding of our study is that mobile lipids accumulate in muscle tissue in response to injury (Fig. 3 and Table I). These findings support the hypothesis that trauma leads to insulin resistance. Indeed, insulin resistance has been suggested to develop following critical illness and severe injury (46). Elevated IMCL levels have been associated with insulin resistance, a major metabolic dysfunction of diabetes (47,48), aging (6,48-50), burn trauma (32-36) and obesity (51-54). Previous genomic (55) and gene expression data in studies of human diabetics (56) suggest that elevated IMCL levels are the result of a deficiency in mitochondrial oxidative capacity (56,57), suggesting that an elevated IMCL content is indicative of reduced mitochondrial oxidation and phosphorylation.

Another principal finding of the present study was that ceramide had accumulated in aged injured flies (Table I and Fig. 3), to a greater extent than in young injured flies, as we have previously shown (34). Ceramide accumulation decreases insulin- stimulated glucose transporter type 4 (GLUT4) translocation to the plasma membrane, which results in decreased glucose transport and, consequently, in the development of insulin resistance. Paumen *et al* demonstrated that saturated fatty acids (e.g., palmitoleic acid, signal at 2.02 ppm in our study) induced the *de novo* synthesis of ceramide and programmed cell death (58); they suggested that the inhibition of carnitine palmitoyl transferase I activity induced both sphingolipid synthesis and palmitate-induced cell death. Moreover, Ruddock *et al* (59) suggested that long-chain saturated fatty acids (e.g., palmitoleic acid C16:0) inhibited insulin activity and

attenuated insulin signal transduction in hepatoma cells, and concluded that an increase in palmitoleic acid is a harbinger of insulin resistance. If so, the signal at 2.02 ppm, which was high in the aged flies in our study, could be a biomarker of insulin resistance. Our NMR data further suggest that trauma induces the activation of the sphingolipid pathway, including ceramide, which functions as an intracellular apoptosis signal. Indeed, our data demonstrated vinyl proton accumulation at 5.33 ppm (Table I), including protons from ceramide and possibly other sphingolipids, such as sphingosine and other monounsaturated fatty acids. These enhanced signals are in accordance with the hypothesis that the sphingolipid pathway may contribute to trauma-mediated apoptosis (60,61).

Of note, SS-31-treated flies exhibited a significantly reduced 5.33-ppm resonance in our study (Table I, Fig. 3), which supports our prior finding that SS-31 promotes mitochondrial respiration and inhibits ROS production (62). SS-31 inhibits cardiolipin peroxidation and mitochondrial permeability transition, thus preventing the release of cytochrome *c* and consequent apoptosis (62,63), and SS-31 has been shown to promote mitochondrial bioenergetics in skeletal muscle and prevent insulin resistance (64-67).

SS-31 has been reported to improve mitochondrial respiration in skeletal muscle, reduce ROS production following immobilization, and prevent the development of insulin resistance (64,65,68). Consistent with our prior findings on mouse burn trauma (8), our complementary EPR results confirm that trauma-induced changes occurred in the redox status, and that SS-31 facilitated the normalization of the mitochondrial redox status in injured flies (Table I, Fig. 5). SS-31 targets and concentrates in the inner mitochondrial membrane, where it reduces mitochondrial oxidative stress via several mechanisms: it can scavenge electrons directly via its dimethyltyrosine residue (69), reduce mitochondrial ROS activity (64,68) and prevent cardiolipin peroxidation elicited by the cardiolipin/cytochrome *c* complex (62). Cardiolipin peroxidation triggers mitochondrial permeability transition, and SS-31 has been reported to inhibit mitochondrial permeability transition and swelling and apoptosis (69). The ability of SS-31 to inhibit insulin resistance induced by a high fat diet (65) and burn trauma (66) may be a result of its protective effect on mitochondrial function.

Trauma can induce lipid peroxidation, a biomarker of lipid damage from oxidative stress (70). Indeed, trauma-induced free radicals can attack intra-membrane PUFAs, which our NMR data revealed to be elevated in injured flies (see CH_2CO resonance at 0.24 ppm in Table I) to form lipid peroxides which can disrupt membrane permeability, integrity and function, compromise cellular components, and lead to further injury (71,72). Our use of EPR spectroscopy to analyze trauma-related oxidative damage and lipid peroxidation in *Drosophila*, allowed us to corroborate previously described protective effects of SS-31 against lipid peroxidation (63,73,74).

In the present study, we demonstrated that the innovative approach of employing *in vivo* HRMAS NMR complemented by EPR spectroscopy is a sensitive method for characterizing metabolic and mitochondrial perturbations in injured *Drosophila* at the molecular level. Furthermore, we demonstrated that SS-31 can reverse injury-induced mitochondrial dysfunction and associated insulin resistance (75), as evidenced by NMR, while also attenuating injury-induced oxidative stress effects, as evidenced by EPR. The relative timing and interactions of SS-31 warrant further investigations in which the constituent events are isolated.

As corollary benefits, our approach advances the development of non-invasive *in vivo* research approaches in *Drosophila*, offers biomarkers which may be used to investigate biomedical paradigms, and thus may direct novel mitochondrial therapeutic development. Our demonstration of the utility of this approach in the extraordinarily well characterized and practicable model organism *D. melanogaster* can pave the way for a shift in the current research paradigm in trauma. Given that our findings are relevant for the treatment of mitochondrial dysfunction that occurs in as many chronic and terminal diseases as in trauma, this study is of great relevance to public health.

Acknowledgements

The present study was supported in part by a grant from DM103014 of the Defense Medical Research and Development Program (DMRDP) to Laurence G. Rahme (Aria A. Tzika, co-investigator), and Shriner's Hospital for Children research grants to Aria A. Tzika (no. 8893) and Laurence G. Rahme (no. 8892). The authors also thank Dr Ann Power Smith (Write Science Right, Las Vegas, NV, USA) for providing editorial assistance. The SS peptide technology has been licensed for commercial development to Stealth Peptides Inc. by the Cornell Research Foundation (CRF), and both CRF and Hazel H. Szeto have financial interests. We would also like to thank Dr Robert Perrimon for providing the *chico* flies.

References

1. Sobrino J and Shafi S: Timing and causes of death after injuries. Proc (Bayl Univ Med Cent) 26: 120-123, 2013.
2. López-Lluch G, Irusta PM, Navas P and de Cabo R: Mitochondrial biogenesis and healthy aging. Exp Gerontol 43: 813-819, 2008.
3. Poulose N and Raju R: Aging and injury: alterations in cellular energetics and organ function. Aging Dis 5: 101-108, 2014.
4. Hubbard WJ, Bland KI and Chaudry IH: The role of the mitochondrion in trauma and shock. Shock 22: 395-402, 2004.
5. Jacob S, Machann J, Rett K, Brechtel K, Volk A, Renn W, Maerker E, Matthaei S, Schick F, Claussen CD and Häring HU: Association of increased intramyocellular lipid content with insulin resistance in lean nondiabetic offspring of type 2 diabetic subjects. Diabetes 48: 1113-1119, 1999.
6. Petersen KF, Befroy D, Dufour S, Dziura J, Ariyan C, Rothman DL, DiPietro L, Cline GW and Shulman GI: Mitochondrial dysfunction in the elderly: possible role in insulin resistance. Science 300: 1140-1142, 2003.
7. Weybright P, Millis K, Campbell N, Cory DG and Singer S: Gradient, high-resolution, magic angle spinning 1H nuclear magnetic resonance spectroscopy of intact cells. Magn Reson Med 39: 337-345, 1998.
8. Blankenberg FG, Storrs RW, Naumovski L, Goralski T and Spielman D: Detection of apoptotic cell death by proton nuclear magnetic resonance spectroscopy. Blood 87: 1951-1956, 1996.
9. Cheng LL, Ma MJ, Becerra L, Ptak T, Tracey I, Lackner A and González RG: Quantitative neuropathology by high resolution magic angle spinning proton magnetic resonance spectroscopy. Proc Natl Acad Sci U S A 12: 6408-6413, 1997.
10. Cheng LL, Newell K, Mallory AE, Hyman BT and Gonzalez RG: Quantification of neurons in Alzheimer and control brains with ex vivo high resolution magic angle spinning proton magnetic resonance spectroscopy and stereology. Magn Reson Imaging 20: 527-533, 2002.
11. Millis KK, Maas WE, Cory DG and Singer S: Gradient, high-resolution, magic-angle spinning nuclear magnetic resonance spectroscopy of human adipocyte tissue. Magn Reson Med 38: 399-403, 1997.

12. Barton SJ, Howe FA, Tomlins AM, Cudlip SA, Nicholson JK, Bell BA and Griffiths JR: Comparison of in vivo 1H MRS of human brain tumours with 1H HR-MAS spectroscopy of intact biopsy samples in vitro. MAGMA 8: 121-128, 1999.
13. Alves TC, Jarak I and Carvalho RA: NMR methodologies for studying mitochondrial bioenergetics. Methods Mol Biol 810: 281-309, 2012.
14. Szczepaniak LS, Babcock EE, Schick F, Dobbins RL, Garg A, Burns DK, McGarry JD and Stein DT: Measurement of intracellular triglyceride stores by H spectroscopy: validation in vivo. Am J Physiol 276: E977-E989, 1999.
15. Feala JD, Coquin L, McCulloch AD and Paternostro G: Flexibility in energy metabolism supports hypoxia tolerance in *Drosophila* flight muscle: metabolomic and computational systems analysis. Mol Syst Biol 3: 99, 2007.
16. Pedersen KS, Kristensen TN, Loeschcke V, Petersen BO, Duus JO, Nielsen NC and Malmendal A: metabolomic signatures of inbreeding at benign and stressful temperatures in *Drosophila melanogaster*. Genetics 180: 1233-1243, 2008.
17. Le Bourg E; Le Bourg E: Oxidative stress, aging and longevity in *Drosophila melanogaster*. FEBS Lett 498: 183-186, 2001.
18. Garofalo RS: Genetic analysis of insulin signaling in *Drosophila*. Trends Endocrinol Metab 13: 156-162, 2002.
19. Saltiel AR and Kahn CR: Insulin signalling and the regulation of glucose and lipid metabolism. Nature 414: 799-806, 2001.
20. Szeto HH: First-in-class cardiolipin-protective compound as a therapeutic agent to restore mitochondrial bioenergetics. Br J Pharmacol 171: 2029-2050, 2014.
21. Apidianakis Y, Mindrinos MN, Xiao W, Lau GW, Baldini RL, Davis RW and Rahme LG: Profiling early infection responses: *Pseudomonas aeruginosa* eludes host defenses by suppressing antimicrobial peptide gene expression. Proc Natl Acad Sci USA 102: 2573-2578, 2005.
22. Apidianakis Y and Rahme LG: *Drosophila melanogaster* as a model host for studying *Pseudomonas aeruginosa* infection. Nat Protoc 4: 1285-1294, 2009.
23. Böhni R, Riesgo-Escovar J, Oldham S, Brogiolo W, Stocker H, Andruss BF, Beckingham K and Hafen E: Autonomous control of cell and organ size by CHICO, a *Drosophila* homolog of vertebrate IRS1-4. Cell 97: 865-875, 1999.
24. Meiboom S and Gill D: Modified spiin-echo method for measuring nuclear relaxation time. Rev Sci Instrum 29: 688-691, 1958.
25. Levenberg K: Method for the solution of certain non-linear problems in least squares. Q Appl Math 2: 164-168, 1944.
26. Marquardt D: An algorithm for least-squares estimation of nonlinear parameters. SIAM J Appl Math 11: 431-441, 1963.
27. Swanson MG, Zektzer AS, Tabatabai ZL, Simko J, Jarso S, Keshari KR, Schmitt L, Carroll PR, Shinohara K, Vigneron DB and Kurhanewicz J: Quantitative analysis of prostate metabolites using 1H HR-MAS spectroscopy. Magn Reson Med 55: 1257-1264, 2006.
28. Khan N and Das DK: Application of in vivo EPR for tissue pO_2 and redox measurements. Methods Mol Biol 559: 131-139, 2009.
29. Swartz HM, Khan N and Khramtsov VV: Use of electron paramagnetic resonance spectroscopy to evaluate the redox state in vivo. Antioxid Redox Signal 9: 1757-1771, 2007.
30. Khan N, Mupparaju SP, Mintzopoulos D, Kesarwani M, Righi V, Rahme LG, Swartz HM and Tzika AA: Burn trauma in skeletal muscle results in oxidative stress as assessed by in vivo electron paramagnetic resonance. Mol Med Rep 1: 813-819, 2008.
31. Padfield KE, Astrakas LG, Zhang Q, Gopalan S, Dai G, Mindrinos MN, Tompkins RG, Rahme LG and Tzika AA: Burn injury causes mitochondrial dysfunction in skeletal muscle. Proc Natl Acad Sci USA 102: 5368-5373, 2005.
32. Zhang Q, Cao H, Astrakas LG, Mintzopoulos D, Mindrinos MN, Schulz J III, Tompkins RG, Rahme LG and Tzika AA: Uncoupling protein 3 expression and intramyocellular lipid accumulation by NMR following local burn trauma. Int J Mol Med 18: 1223-1229, 2006.
33. Tzika AA, Astrakas LG, Cao H, Mintzopoulos D, Zhang Q, Padfield K, Yu H, Mindrinos MN, Rahme LG and Tompkins RG: Murine intramyocellular lipids quantified by NMR act as metabolic biomarkers in burn trauma. Int J Mol Med 21: 825-832, 2008.
34. Righi V, Apidianakis Y, Mintzopoulos D, Astrakas L, Rahme LG and Tzika AA: *In vivo* high-resolution magic angle spinning magnetic resonance spectroscopy of *Drosophila melanogaster* at 14.1 T shows trauma in aging and in innate immune-deficiency is linked to reduced insulin signaling. Int J Mol Med 26: 175-184, 2010.
35. Astrakas LG, Goljer I, Yasuhara S, Padfield KE, Zhang Q, Gopalan S, Mindrinos MN, Dai G, Yu YM, Martyn JA, *et al*: Proton NMR spectroscopy shows lipids accumulate in skeletal muscle in response to burn trauma-induced apoptosis. FASEB J 19: 1431-1440, 2005.
36. Weis J, Johansson L, Ortiz-Nieto F and Ahlström H: Assessment of lipids in skeletal muscle by LCModel and AMARES. J Magn Reson Imaging 30: 1124-1129, 2009.
37. Wang L, Salibi N, Wu Y, Schweitzer ME and Regatte RR: Relaxation times of skeletal muscle metabolites at 7T. J Magn Reson Imaging 29: 1457-1464, 2009.
38. Griffin JL, Williams HJ, Sang E and Nicholson JK: Abnormal lipid profile of dystrophic cardiac tissue as demonstrated by one- and two-dimensional magic-angle spinning (1)H NMR spectroscopy. Magn Reson Med 46: 249-255, 2001.
39. Chen JH, Sambol EB, Decarolis P, O'Connor R, Geha RC, Wu YV and Singer S: High-resolution MAS NMR spectroscopy detection of the spin magnetization exchange by cross-relaxation and chemical exchange in intact cell lines and human tissue specimens. Magn Reson Med 55: 1246-1256, 2006.
40. Tiefenböck SK, Baltzer C, Egli NA and Frei C: The *Drosophila* PGC-1 homologue Spargel coordinates mitochondrial activity to insulin signalling. EMBO J 29: 171-183, 2010.
41. Baltzer C, Tiefenböck SK, Marti M and Frei C: Nutrition controls mitochondrial biogenesis in the *Drosophila* adipose tissue through Delg and cyclin D/Cdk4. PLoS One 4: e6935, 2009.
42. Padfield KE, Zhang Q, Gopalan S, Tzika AA, Mindrinos MN, Tompkins RG and Rahme LG: Local and distant burn injury alter immuno-inflammatory gene expression in skeletal muscle. J Trauma 61: 280-292, 2006.
43. Tzika AA, Mintzopoulos D, Padfield K, Wilhelmy J, Mindrinos MN, Yu H, Cao H, Zhang Q, Astrakas LG, Zhang J, *et al*: Reduced rate of adenosine triphosphate synthesis by *in vivo* 31P nuclear magnetic resonance spectroscopy and downregulation of PGC-1β in distal skeletal muscle following burn. Int J Mol Med 21: 201-208, 2008.
44. Righi V, Andronesi O, Mintzopoulos D and Tzika AA: Molecular characterization and quantification using state of the art solid-state adiabatic TOBSY NMR in burn trauma. Int J Mol Med 24: 749-757, 2009.
45. Tzika AA, Mintzopoulos D, Mindrinos M, Zhang J, Rahme LG and Tompkins RG: Microarray analysis suggests that burn injury results in mitochondrial dysfunction in human skeletal muscle. Int J Mol Med 24: 387-392, 2009.
46. Thompson LH, Kim HT, Ma Y, Kokorina NA and Messina JL: Acute, muscle-type specific insulin resistance following injury. Mol Med 14: 715-723, 2008.
47. Machann J, Thamer C, Schnoedt B, Stefan N, Stumvoll M, Haring HU, Claussen CD, Fritsche A and Schick F: Age and gender related effects on adipose tissue compartments of subjects with increased risk for type 2 diabetes: a whole body MRI/MRS study. MAGMA 18: 128-137, 2005.
48. Nakagawa Y, Hattori M, Harada K, Shirase R, Bando M and Okano G: Age-related changes in intramyocellular lipid in humans by in vivo H-MR spectroscopy. Gerontology 53: 218-223, 2007.
49. Rouffet D, Villars C, Fissoune R, Sappey-Marinier D, Laville M, Ibarrola D, Sothier M, Monnet MF, Ovize M, Bonnefoy M, *et al*: Intramyocellular lipid variations in active older men: relationship with aerobic fitness. Acta Physiol (Oxf) 207: 516-523, 2013.
50. Petersen KF, Morino K, Alves TC, Kibbey RG, Dufour S, Sono S, Yoo PS, Cline GW and Shulman GI: . Effect of aging on muscle mitochondrial substrate utilization in humans. Proc Natl Acad Sci USA 112: 11330-11334, 2015.
51. Sinha R, Dufour S, Petersen KF, LeBon V, Enoksson S, Ma YZ, Savoye M, Rothman DL, Shulman GI and Caprio S: Assessment of skeletal muscle triglyceride content by (1)H nuclear magnetic resonance spectroscopy in lean and obese adolescents: relationships to insulin sensitivity, total body fat, and central adiposity. Diabetes 51: 1022-1027, 2002.
52. Schrauwen-Hinderling VB, Hesselink MK, Schrauwen P and Kooi ME: Intramyocellular lipid content in human skeletal muscle. Obesity (Silver Spring) 14: 357-367, 2006.
53. Consitt LA, Bell JA and Houmard JA: Intramuscular lipid metabolism, insulin action, and obesity. IUBMB Life 61: 47-55, 2009.
54. Johnson AB, Argyraki M, Thow JC, Cooper BG, Fulcher G and Taylor R: Effect of increased free fatty acid supply on glucose metabolism and skeletal muscle glycogen synthase activity in normal man. Clin Sci (Lond) 82: 219-226, 1992.

55. Mootha VK, Bunkenborg J, Olsen JV, Hjerrild M, Wisniewski JR, Stahl E, Bolouri MS, Ray HN, Sihag S, Kamal M, *et al*: Integrated analysis of protein composition, tissue diversity, and gene regulation in mouse mitochondria. Cell 115: 629-640, 2003.
56. Petersen KF, Dufour S, Befroy D, Garcia R and Shulman GI: Impaired mitochondrial activity in the insulin-resistant offspring of patients with type 2 diabetes. N Engl J Med 350: 664-671, 2004.
57. Patti ME, Butte AJ, Crunkhorn S, Cusi K, Berria R, Kashyap S, Miyazaki Y, Kohane I, Costello M, Saccone R, *et al*: Coordinated reduction of genes of oxidative metabolism in humans with insulin resistance and diabetes: potential role of PGC1 and NRF1. Proc Natl Acad Sci USA 100: 8466-8471, 2003.
58. Paumen MB, Ishida Y, Muramatsu M, Yamamoto M and Honjo T: Inhibition of carnitine palmitoyltransferase I augments sphingolipid synthesis and palmitate-induced apoptosis. J Biol Chem 272: 3324-3329, 1997.
59. Ruddock MW, Stein A, Landaker E, Park J, Cooksey RC, McClain D and Patti ME: Saturated fatty acids inhibit hepatic insulin action by modulating insulin receptor expression and post-receptor signalling. J Biochem 144: 599-607, 2008.
60. Yasuhara S, Perez ME, Kanakubo E, Yasuhara Y, Shin YS, Kaneki M, Fujita T and Martyn JA: Skeletal muscle apoptosis after burns is associated with activation of proapoptotic signals. Am J Physiol Endocrinol Metab 279: E1114-E1121, 2000.
61. Tomera JF and Martyn J: Systemic effects of single hindlimb burn injury on skeletal muscle function and cyclic nucleotide levels in the murine model. Burns 14: 210-219, 1988.
62. Birk AV, Liu S, Soong Y, Mills W, Singh P, Warren JD, Seshan SV, Pardee JD and Szeto HH: The mitochondrial-targeted compound SS-31 re-energizes ischemic mitochondria by interacting with cardiolipin. J Am Soc Nephrol 24: 1250-1261, 2013.
63. Szeto HH: Cell-permeable, mitochondrial-targeted, peptide antioxidants. AAPS J 8: E277-E283, 2006.
64. Min K, Smuder AJ, Kwon OS, Kavazis AN, Szeto HH and Powers SK: Mitochondrial-targeted antioxidants protect skeletal muscle against immobilization-induced muscle atrophy. J Appl Physiol 1985 111: 1459-1466, 2011.
65. Anderson EJ, Lustig ME, Boyle KE, Woodlief TL, Kane DA, Lin CT, Price JW III, Kang L, Rabinovitch PS, Szeto HH, *et al*: Mitochondrial H_2O_2 emission and cellular redox state link excess fat intake to insulin resistance in both rodents and humans. J Clin Invest 119: 573-581, 2009.
66. Carter EA, Bonab AA, Goverman J, Paul K, Yerxa J, Tompkins RG and Fischman AJ: Evaluation of the antioxidant peptide SS31 for treatment of burn-induced insulin resistance. Int J Mol Med 28: 589-594, 2011.
67. Siegel MP, Kruse SE, Percival JM, Goh J, White CC, Hopkins HC, Kavanagh TJ, Szeto HH, Rabinovitch PS and Marcinek DJ: Mitochondrial-targeted peptide rapidly improves mitochondrial energetics and skeletal muscle performance in aged mice. Aging Cell 12: 763-771, 2013.
68. Powers SK, Hudson MB, Nelson WB, Talbert EE, Min K, Szeto HH, Kavazis AN and Smuder AJ: Mitochondria-targeted antioxidants protect against mechanical ventilation-induced diaphragm weakness. Crit Care Med 39: 1749-1759, 2011.
69. Zhao K, Zhao GM, Wu D, Soong Y, Birk AV, Schiller PW and Szeto HH: Cell-permeable peptide antioxidants targeted to inner mitochondrial membrane inhibit mitochondrial swelling, oxidative cell death, and reperfusion injury. J Biol Chem 279: 34682-34690, 2004.
70. Smith JA, Park S, Krause JS and Banik NL: Oxidative stress, DNA damage, and the telomeric complex as therapeutic targets in acute neurodegeneration. Neurochem Int 62: 764-775, 2013.
71. Ozkur MK, Bozkurt MS, Balabanli B, Aricioglu A, Ilter N, Gürer MA and Inalöz HS: The effects of EGb 761 on lipid peroxide levels and superoxide dismutase activity in sunburn. Photodermatol Photoimmunol Photomed 18: 117-120, 2002.
72. Akeo K, Amaki S, Suzuki T and Hiramitsu T: Melanin granules prevent the cytotoxic effects of L-DOPA on retinal pigment epithelial cells in vitro by regulation of NO and superoxide radicals. Pigment Cell Res 13: 80-88, 2000.
73. Szeto HH: Mitochondria-targeted peptide antioxidants: novel neuroprotective agents. AAPS J 8: E521-E531, 2006.
74. Szeto HH: Development of mitochondria-targeted aromatic-cationic peptides for neurodegenerative diseases. Ann N Y Acad Sci 1147: 112-121, 2008.
75. Lowell BB and Shulman GI: Mitochondrial dysfunction and type 2 diabetes. Science 307: 384-387, 2005.